Pathology - Research and Practice 215 (2019) 358–365

Contents lists available at ScienceDirect

Pathology - Research and Practice

journal homepage: www.elsevier.com/locate/prp

FBXL3 is regulated by miRNA-4735-3p and suppresses cell proliferation and migration in non-small cell lung cancer

Dazhong Wang, Xin Han, Chan Li, Weijun Bai*

Third Medical Oncology Department of Thoracic Cancer, Cancer Hospital of China Medical University, Liaoning Cancer Hospital & Institute, No. 44, Xiaoheyan road, Dadong district, Shenyang city, Liaoning province, 110042, China

ARTICLE INFO

Keywords:
FBXL3
miR-4735-3p
Non-small cell lung cancer
Proliferation

ABSTRACT

Non-small cell lung cancer (NSCLC) is the most common type of primary lung cancer and regarded as cancer killer. The aim of this study was to discover the detailed function and molecular mechanism of F-box and leucine rich repeat protein 3 (FBXL3) in NSCLC. In this study, the expression level of FBXL3 in NSCLC tissues and cell lines was firstly examined and identified. Moreover, the relationship between FBXL3 and the overall survival rate of NSCLC patients was analyzed by Kaplan–Meier survival curve. Functionally, MTT, colony formation assay and transwell assays were performed to determine the role of FBXL3 in regulating NSCLC cell proliferation, migration and invasion. The proliferation and migration were suppressed by overexpression of FBXL3, indicating the potential tumor suppressive role of FBXL3 in NSCLC. In addition, the dual-luciferase reporter and RNA pull-down assays revealed that miR-4735-3p was a novel upstream modulator of FBXL3. Further study showed that miR-4735-3p was upregulated in NSCLC tissues and cell lines. Finally, rescue assays and function assays revealed that miR-4735-3p exerted oncogenic function in NSCLC, and this function can be attenuated by FBXL3. Taken together, FBXL3 was regulated by miR-4735-3p and suppressed cell proliferation and invasion in non-small cell lung cancer.

1. Introduction

As one of the most common malignancies, lung cancer has become the leading cause of cancer-related death all over the world [4,27]. Non-small cell lung cancer (NSCLC) accounts for approximately 80% among all types of lung cancer [11]. Non-small cell lung cancer is commonly classified into two subtypes, squamous cell carcinoma and adenocarcinoma cell carcinoma [29]. Although, advances have been made in the chemotherapy and molecular targeting therapy, the overall 5-year survival rate for NSCLC patients is still low [31]. Therefore, it is critical to find the diagnostic markers and effective therapeutic targets for NSCLC.

The currently developed treatment method was miRNAs-mediated translational suppression of mRNAs, which led to gene silencing at mRNA level [6]. F-box and leucine rich repeat protein 3 (FBXL3) has been reported to be downregulated in colorectal cancer, and acted as a target gene of miRNA [10]. MicroRNAs (miRNAs) are small non-coding RNA and consist of 21–23 nucleotides [16]. Increasing studies have documented that miRNAs exert its role in posttranscriptional level via changing the translation of mRNA [3,26]. Reports also demonstrated the effects of miRNAs on gene expression and biological processes in different types of cancers [12,15]. Some miRNAs participated in the development and progression of NSCLC via suppressing or degrading the expression of their targets [2,14,32,33]. These reports suggested miRNAs can act as an upstream gene of mRNA and regulate mRNA expression. However, little was known about FBXL3 and its correlation with miRNA in NSCLC. Thus, this study aims to explore the interaction between FBXL3 and miR-4735-3p and their functions in NSCLC.

2. Materials and methods

2.1. Tissue samples

All tissue samples (NSCLC tissues, n = 80; adjacent normal tissues, n = 80) were collected from NSCLC patients in the Third Medical Oncology Department of Thoracic Cancer, Liaoning Cancer Hospital & Institute. This study was approved by the ethics committee of Cancer Hospital of Liaoning Cancer Hospital & Institute. The informed consents had been obtained from all patients.

* Corresponding author.
E-mail address: Weijunbaaa_356@163.com (W. Bai).

https://doi.org/10.1016/j.prp.2018.12.008
Received 25 July 2018; Received in revised form 20 November 2018; Accepted 9 December 2018

2.2. Cell culture

Four NSCLC cell lines (NCL-H460, NCL-H358, NCL-H1299 and NCL-H146) and one normal bronchial epithelial cell line (16HBE) were purchased from the Institute of Biochemistry and Cell Biology of the Chinese Academy of Sciences (Shanghai, China). Cell lines were maintained in DMEM medium (GIBCO-BRL) and supplemented with 10% fetal bovine serum (FBS, Sigma, San Francisco, CA, USA), 100 U/ml of penicillin and 100 μg/ml of streptomycin (Sigma). Cell lines were cultured in a humidified atmosphere at 37 °C with 5% CO_2.

2.3. Plasmid construction

The pcDNA-FBXL3 vector and specific siRNA against FBXL3 vector were synthesized by GenePharma (Shanghai, China). MiR-4735-3p mimics, miR-4735-3p inhibitor (anti-miR-4735-3p) and their negative control (miR-NC or anti-NC) were synthesized from GenePharma (Shanghai, China). According to the recommendation of manufacturer, LipofectamineTM 2000 reagent (Invitrogen, Carlsbad, CA, USA) was used to transfect all plasmids into NCL-H460 and NCL-H1299 cells. The sequence of miR-4735-3p inhibitor: UUUCCACGAGUUUAAUCUGUA. The miR-4735-3p mimics sequence: AAAGGUGCUCAAAUUAGACAU. The miR-NC sequence: CGGUUCGCTAGCGCCGACUCG. The anti-NC sequence: CAGUACUUUUGUGUAGUACAA.

2.4. RNA isolation and qRT-PCR

Total mRNAs were extracted from NSCLC cells by using TRIzol reagent (Qiagen, Dusseldorf, Germany). Subsequently, reverse transcription was conducted by TaqMan® MicroRNA Reverse Transcription Kit (Life technologies). The synthesis of complementary DNA (cDNA) was performed using Oligo (dT). The SYBR Premix Ex TaqTM Kit (TaKaRa, Tokyo, Japan) was used for Real-time PCR. The amplification parameters were: 95 °C for 5 min, 40 cycles of 95 °C for 30 s, 60 °C for 30 s and 72 °C for 1 min, following the final extension was 72 °C for 5 min. The results were calculated with the $2^{-\Delta\Delta Ct}$ method and normalized to GAPDH. The primers for real-time PCR were showed as followings: FBXL3 (forward), 5′-AGACCTTGGAGCTTGCTTGG-3′, FBXL3 (reverse), 5′−CCTGGGCAGTTTGCTTTGAC-3′; miR-4735-3p (forward), 5′-GAAG GTGCTCAAACCAGACAT-3′, miR-4735-3p (reverse), 5′- CTCTACAGCT ATATTGCCAGCCA-3′; GAPDH (forward), 5′-AACAGGAGGTCCCTACT CCC-3′, GAPDH (reverse), 5′-GCCATTTTGCGGTGGAAATG-3′; U6 (forward), 5′-GCAGACCGTTCGTCAACCTA-3′, U6 (reverse), 5′-AATTCTGT TTGCGGTGCGTC-3′.

2.5. Cell viability assay

MTT (Sigma-Aldrich, St. Louis, MI, USA) assay was carried out to detect the cell viability. Briefly, NCL-H460 and NCL-H1299 cell lines were seeded into 96-well plates at a density of 4×10^3 cells/well. NCL-H460 and NCL-H1299 cells were transfected with FBXL3 or NC with different time stage (24, 48, 72, 96 h). Cell viability was assessed by observing the absorbance at 490 nm for each well using a microplate spectrophotometer.

2.6. Colony formation assay

After transfection, NCL-H460 and NCL-H1299 cell lines were plated in the 6-well plates at a density of 1×10^3/100 μL, following an incubation at 37 °C in a humidified atmosphere with 5% CO_2. After two weeks, cells were treated with phosphate buffered saline (PBS, Invitrogen, CA, USA). The colonies were fixed with 4% paraformaldehyde for 30 min and dyed with 0.1% crystal violet for 15 min. Subsequently, the colonies were washed three times with PBS. At last, the pictures of plates were taken. The stained colonies were counted manually.

2.7. Apoptosis assay

2.7.1. Flow cytometry analyses

48 h post-transfection, NCL-H460 and NCL-H1299 cell lines were reaped and digested with trypsin, followed by low speed centrifugation for 15 min to wipe off the supernatant. Then, cells were washed two times with precooled PBS (Invitrogen, CA, USA) prior to the fixation with 5 ml of 70% pre-iced ethanol at 4 °C overnight. Thereafter, the fixed cells were stained with propidium iodide (PI, Sigma-Aldrich; San Francisco, CA, USA) in the presence of Ribonuclease A (BD Biosciences, San Diego, CA, USA) at 4 °C for 30 min in the dark. The cell cycle distributions in the G0/G1, S, and G2/M phases were detected and analyzed via FACScan (Beckman Coulter, Mansfield, MA, USA) and FlowJo software (Treestar, Inc., Ashland, OR, USA) in accordance with the standard method.

Apoptosis analysis were conducted by using Annexin V-FITC/PI Apoptosis Detection Kit (Sigma-Aldrich). After transfection, NCL-H460 and NCL-H1299 cell lines (2×10^4 /mL) were harvested and washed 3 times in PBS. Thereafter, cells were cultured in 70% cold ethanol for 1 h on ice and dyed with 200 μL of binding buffer, which containing 10 μL Annexin V-FITC and 5 μL of PI. After incubation for 1 h in the dark at room temperature, FACScan and FlowJo software were used to analyze cell apoptosis.

2.7.2. Cell migration and invasion assays

After 48 h transfection, NCL-H460 and NCL-H1299 cells were collected and cultured in serum-free culture medium for twelve hours, followed by digestion. Subsequent to washing three times with PBS (Invitrogen), cells were suspended in the serum-free DMEM containing 10 mg/L of FBS. The concentration of cell suspension was adjusted to 2×10^6 cells/mL. Cell migration and invasion were detected using a 24-well plate transwell chamber (8 um pore size, Corning, NY, USA) which was pre-coated with (for invasion) or without (for migration) Matrigel (Sigma-Aldrich Chemical Company, St Louis, MO, USA). 48 h later, 200 μL of cells in serum-free medium were added into the upper chamber. 500 μL of medium containing 10% FBS was placed into the lower chamber. Following 48 h incubation at 37 °C with 5% CO_2, cells in the upper membrane were wiped off, while cells that migrated into the lower chamber were fixed in methanol and stained with 0.1% crystal violet. These migratory cells were imaged and counted under an inverted optical microscope (magnification × 100; Olympus Corporation, Tokyo, Japan) through selecting 5 random fields.

2.7.3. Luciferase reporter assay

The wild-type (WT) or mutant (MUT) 3′UTR of FBXL3 containing the predicted miR-4735-3p binding sites was cloned into the pRL-TK vectors. Then, 100 ng of pRL-TK-3′UTR-wt or mutant and 20 ng of pGL3.0 control vector were co-transfected into NCL-H460 and NCL-H1299 cells which were planted in 24 well plate. After 4 h transfection, 50 nM of miR-4735-3p mimic or miR-NC was transfected into NSCLC cells, respectively. The luciferase activities in each cell line were analyzed by dual luciferase assay kit (Promega, Madison, USA).

2.7.4. RNA pull-down assay

In brief, miR-4735-3p, miR-4735-3p-Mut, mimics-NC were separately biotinylated to be Bio-miR-4735-3p-wt, Bio-miR-4735-3p-mut and Bio-NC by GenePharma Company (Shanghai, China). Then, they were transfected into NCL-H460 and NCL-H1299 cells. After 48 h transfection, NCL-H460 and NCL-H1299 cells were collected and lysed. At last, they were incubated with Dynabeads M-280 Streptavidin (Invitrogen, CA) for 10 min and washed with buffer. The bound RNAs were quantified and analyzed by qRT-PCR. The primers were listed as follows: Bio-miR-4735-3p (forward), 5′-GAAGGTGCTCAAACCAGA CAT-3′, Bio-miR-4735-3p (reverse), 5′- CTCTACAGCTATATTGCCAG CCA-3′; Bio-miR-4735-3p-Mut (forward), 5′-CGCATCACTAGAGCCGAC TAC-3′, Bio-miR-4735-3p-Mut (reverse), 5′- CTCTACAGCTATATTGCC

AGCCA-3′; Bio-NC (forward), 5′−CCCCAAAACCCAAGGACCAA-3′, Bio-NC (reverse), 5′−CCGTCCACGTACCAGTTGAA-3′.

2.7.5. Western blotting assay

In brief, NCL-H460 and NCL-H1299 cells were placed into six-well plates and lysed on ice using RIPA buffer. Then, proteins (50 μg) were separated by SDS-PAGE gel (Thermo Scientific, CA, USA) and transferred onto a polyvinylidene difluoride (PVDF, Millipore, Billerica, MA, USA) membrane. Subsequently, the membranes were incubated with 5% defatted milk for 48 h at room temperature. Anti-FBXL3 (ab96645, Abcam, Cambridge, MA, USA, at 1: 1000 dilution), anti-E-cadherin (ab1416, Abcam, at 1: 1000 dilution), anti-*N*-cadherin (ab18203, Abcam, at 1: 1000 dilution) and anti-GAPDH (ab8245, Abcam, at 1: 1000 dilution) were utilized as the primary antibodies. The secondary antibodies were HRP-conjugated antibodies at 1: 2000 dilution. Membranes were cultured with primary antibodies at 4 °C all night and then with secondary antibodies for two hours at room temperature. Finally, an enhanced chemiluminescence (ECL, Bio-Rad lab, Hercules, CA, USA) was utilized to visualize the protein signals.

2.7.6. Statistical analysis

Statistical analyses were analyzed via using SPSS 17.0 software. Statistical significances were measured by Student's *t*-test and one-way ANOVA. Kaplan–Meier analysis and log rank test were utilized to detect the overall survival rate of NSCLC patients. Cox regression analysis was further applied to analyze prognostic factors. The correlation between FBXL3 and miR-4735-3p was detected by Spearman's correlation analysis. Data represent mean ± standard deviation (SD) of at least three independent experiments. $p < 0.05$ was considered significantly.

3. Results

3.1. FBXL3 was downregulated in NSCLC tissues and cell lines

To explore the role of FBXL3 in the NSCLC, qRT-PCR assay was firstly conducted to measure the expression level of FBXL3 in 80 pairs of NSCLC tissues and corresponding normal tissues. Results revealed that FBXL3 expression was significantly downregulated in cancer tissues compared with normal tissues (Fig. 1A). In addition, we analyzed the expression levels of FBXL3 in four NSCLC cell lines (NCL-H460, NCL-H358, NCL-H1299 and A549) and one normal bronchial epithelial cell line (16HBE). The expression levels of FBXL3 was significantly decreased in NSCLC cell lines, especially in NCL-H460 and NCL-H1299 cells (Fig. 1B). The mean value of the expression level of FBXL3 in NSCLC tissues was used as a diving line. We divided all samples into two groups (high expression group and low expression group). Then, we assessed the correlation between FBXL3 expression and the clinicpathological features of 80 NSCLC patients. The expression level of FBXL3 was associated with TNM stage (p = 0.024), but not with smoking, lymph node metastasis and age as well as gender (Table 1). In addition, these prognostic factors were further detected by Cox regression analysis. The result showed that FBXL3 expression and TNM stage were two independent prognostic factors for NSCLC patients (Table 2). Furthermore, Kaplan–Meier analysis validated that high level of FBXL3 indicated higher overall survival rate compared with those with low level of FBXL3 (Fig. 1C). Collectively, these findings indicated that FBXL3 expression might be correlated with NSCLC progression.

Table 1
Correlation between the expression of FBXL3 and clinicopathological features of NSCLC patients. (n = 80).

Variable	FBXL3 Expression		P-value
	Low	High	
Age			
< 60	17	31	0.810
≥60	10	22	
Gender			
Male	20	36	0.241
Female	7	17	
Lymph Node Metastasis			
Negative	12	20	0.632
Positive	15	33	
Smoking			
No	19	39	0.795
Yes	8	14	
TNM Stage			
I–II	14	41	0.024*
III–IV	13	12	

Low/high by the mean expression of FBXL3. Pearson χ^2 test.
* $p < 0.05$ was considered statistically significant.

3.2. Overexpression of FBXL3 suppressed NSCLC cell proliferation by regulating cell cycle progress and cell apoptosis

To investigate the biological function of FBXL3 in NSCLC, gain-of-function experiments were conducted. qRT-PCR showed that the expression level of FBXL3 was significantly increased in NCL-H460 and NCL-H1299 cells transfected with pcDNA-FBXL3 (Fig. 2A). MTT assay revealed that upregulated FBXL3 obviously suppressed cell viability in NCL-H460 and NCL-H1299 cells (Fig. 2B). Consistent with MTT, colony formation assay demonstrated that overexpression of FBXL3 significantly reduced the colony numbers in NCL-H460 and NCL-H1299 cells (Fig. 2C). Furthermore, we analyzed whether FBXL3 regulated NSCLC cell proliferation via modulation of cell cycle distribution and cell apoptosis. Flow cytometry analysis revealed that FBXL3 overexpression obviously led to cell cycle arrested at G0/G1 phase in both NCL-H460 and NCL-H1299 cells (Fig. 2D). In addition, upregulation of

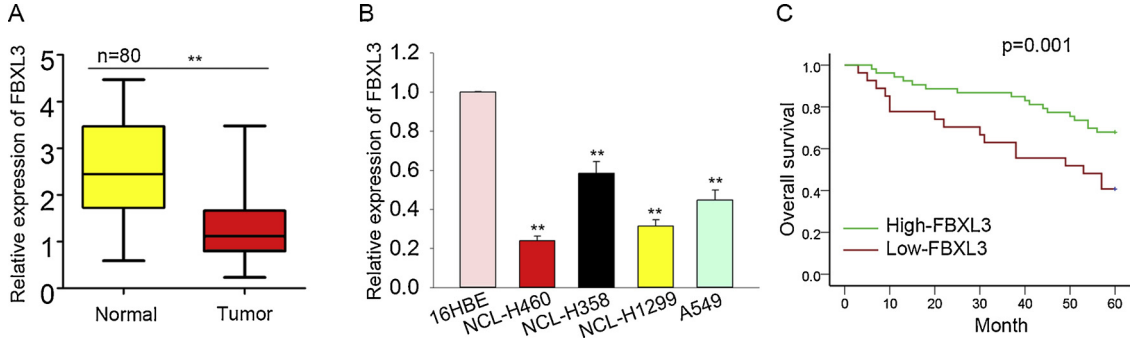

Fig. 1. FBXL3 was downregulated in NSCLC tissues and cell lines. (A) FBXL3 expression was detected by qRT-PCR assay in 80 pairs of NSCLC tissues and adjacent normal tissues. (B) FBXL3 expression was measured by qRT-PCR assay in NSCLC cell lines (NCL-H460, NCL-H358, NCL-H1299 and A549) and one normal bronchial epithelial cell line (16HBE). (C) Kaplan–Meier survival curve and log rank test were utilized to detect the association between FBXL3 expression and overall survival rate of NSCLC patient. * $p < 0.05$; ** $p < 0.01$.

Table 2
Multivariate analysis of prognostic parameters in patients with NSCLC by Cox regression analysis.

Variable	Category	HR(95%CI)	P-value
FBXL3 expression	Low High	0.305(0.15–0.621)	0.001**
Age	< 60 ≥60	0.861(0.418–1.77)	0.686
Gender	Male Female	1.159(0.545–2.46)	0.701
Lymph Node Metastasis	No Yes	1.099(0.522–2.31)	0.803
Smoking	No Yes	1.16(0.538–2.49)	0.705 0.007**
TNM Stage	I–II III–IV	0.278(0.109–0.70)	

Proportional hazards method analysis showed a positive, independent prognostic importance of FBXL3 expression ($p = 0.001$), in addition to TNM stage ($p = 0.007$). $^{**}p < 0.01$ was considered statistically significant.

FBXL3 accelerated NCL-H460 and NCL-H1299 cells apoptosis (Fig. 2E).

3.3. Overexpression of FBXL3 suppressed cell migration, invasion and EMT progress in NSCLC

We further detected whether FBXL3 could affect NSCLC cell migration. Transwell assay showed that overexpressed FBXL3 inhibited cell migration and invasion in both NCL-H460 and NCL-H1299 cell lines (Fig. 3A–B). Additionally, we detected the relative protein level of EMT-related markers, thereby confirming the role of FBXL3 in regulating EMT process. Results suggested that FBXL3 overexpression increased the protein level of E-cadherin, while decreased the level of N-cadherin (Fig. 3C).

3.4. MiR-4735-3p is an upstream modulator of FBXL3 in NSCLC

To detect the underlying molecular mechanism by which FBXL3 regulated NSCLC, we analyzed the potential upstream target genes of FBXL3. 92 upstream miRNAs of FBXL3 were predicted using the online prediction tool starbase (http://starbase.sysu.edu.cn/browseNcRNA.

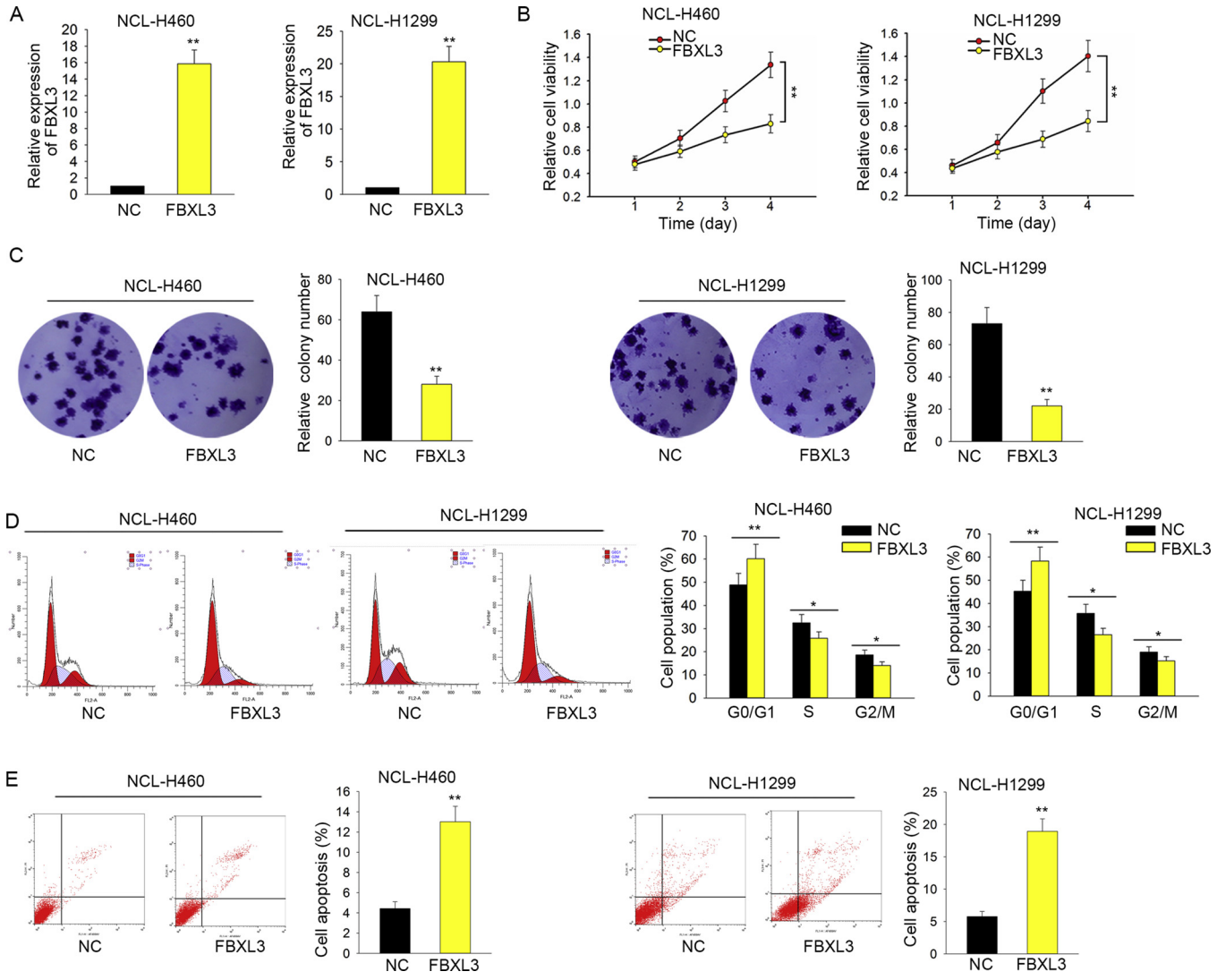

Fig. 2. Overexpression of FBXL3 suppressed NSCLC cell proliferation by regulating cell cycle progress and cell apoptosis. (A) Transfection efficiency were exhibited in both NCL-H460 and NCL-H1299 cells. (B) NCL-H1688 and NCL-H1299 cCell viability were detected by CCK-8 assay after NCL-H460 and NCL-H1299 cells were transfected with NC and pcDNA-FBXL3 (FBXL3). (C) Colony formation ability of NCL-H460 and NCL-H1299 cells transfected with NC and pcDNA-FBXL3 (FBXL3) were examined by colony formation assay. (D–E) Cell cycle and apoptosis were analyzed by flow cytometry analysis after NCL-H460 and NCL-H1299 cells were transfected with NC and pcDNA-FBXL3 (FBXL3). * $p < 0.05$; ** $p < 0.01$.

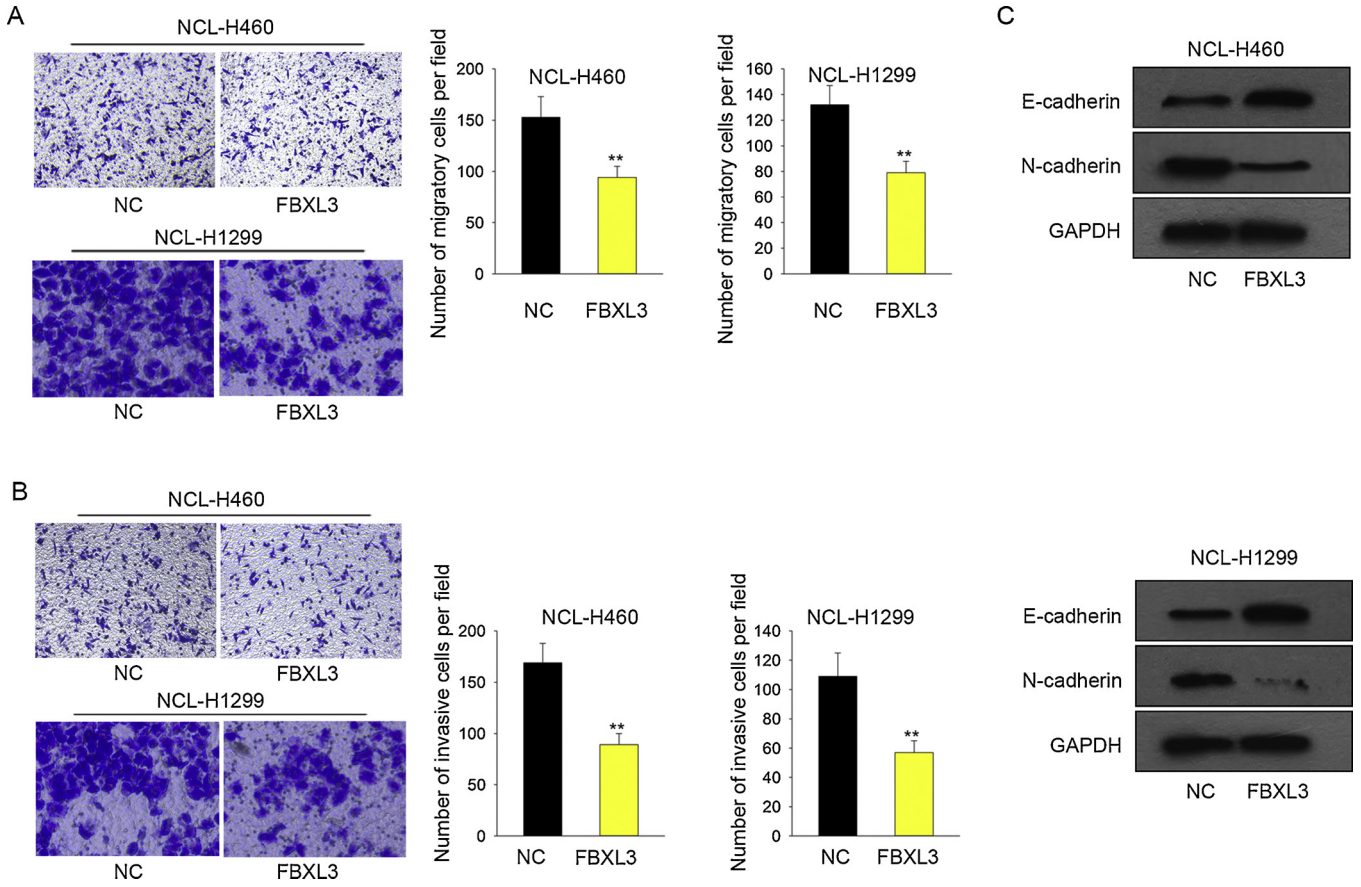

Fig. 3. Overexpression of FBXL3 suppressed cell migration, invasion and EMT progress in NSCLC. (A–B) Transwell assays were performed to analyze cell migration and invasion after NCL-H460 and NCL-H1299 cells were transfected with NC and pcDNA-FBXL3 (FBXL3). (C) Relative protein level of EMT-related markers in NCL-H460 and NCL-H1299 cells were tested by western blot assay. ** $p < 0.01$.

php). Among all these potential miRNAs, only miR-4735-3p has not been studied in NSCLC. Therefore, we chose it for following study. The putative binding site between 3′-UTR of FBXL3 and miR-4735-3p was shown (Fig. 4A). Luciferase reporter assay showed that the luciferase activity was reduced by co-transfecting with miR-4735-3p mimic and wild-type 3′UTR of FBXL3 (FBXL3-WT), while the luciferase activity was not changed when cells were co-transfected with mutant 3′UTR of FBXL3 (FBXL3-MUT) (Fig. 4B). The interaction between miR-4735-3p and FBXL3 was further confirmed by RNA pull-down assay (Fig. 4C). In addition, the expression levels of miR-4735-3p was assessed in NSCLC tissues and cell lines by qRT-PCR assay. Obviously, miR-4735-3p was upregulated in NSCLC tissues and cell lines (Fig. 4D–E). Using the mean value of miR-4735-3p expression as the threshold, the NSCLC samples were classified into miR-4735-3p high expression group and miR-4735-3p low expression group. We then detected the relationship between miR-4735-3p expression and the overall survival rate of NSCLC patients by Kaplan–Meier method. Results demonstrated that higher expression of miR-4735-3p predicted poor overall survival (Fig. 4F). In addition, Spearman's correction analysis revealed that FBXL3 expression was negatively associated with miR-4735-3p expression in NSCLC tissues (Fig. 4G). Then, the regulatory effect of miR-4735-3p on FBXL3 expression was evaluated by qRT-PCR and western blot assay. Results revealed that inhibition of miR-4735-3p increased the mRNA and protein levels of FBXL3, while the levels of FBXL3 were re-decreased by si-FBXL3 (Fig. 4H–I). These data suggested that miR-4735-3p interacted with FBXL3 in NSCLC.

3.5. MiR-4735-3p interacted with FBXL3 to regulate NSCLC progression

To further confirm the role of miR-4735-3p/FBXL3 axis in NSCLC, a series of rescue assays were conducted in NCL-H460 cells. MTT assay and colony formation assay indicated that knockdown of FBXL3 significantly reversed the inhibitory effect of miR-4735-3p inhibition on NSCLC cell proliferation (Fig. 5A–B). In addition, flow cytometry analysis indicated that miR-4735-3p inhibition arrested cell cycle at G0/G1 phase, while co-transfected si-FBXL3 decreased the G0/G1 arrest (Fig. 5C). Moreover, the increased apoptosis induced by miR-4735-3p inhibition was rescued by co-transfecting si-FBXL3 (Fig. 5D). Transwell assay demonstrated cell migration and invasion ability was attenuated by transfecting miR-4735-3p inhibitor into NSCLC cell, but knockdown of FBXL3 remarkably dismissed the inhibitory effect of miR-4735-3p inhibition (Fig. 5E). Furthermore, we treated NCL-H460 cell with miR-NC, miR-4735-3p mimics and FBXL3 expression vector. As presented in Fig. 5F–G, cell proliferation was promoted by miR-4735-3p mimics, which was partially reversed by FBXL3. Furthermore, cell cycle progress promoted by miR-4735-3p was arrested at G0/G1 phase by co-transfection with FBXL3 expression vector (Fig. 5H). Similarly, cell apoptosis rate was decreased by miR-4735-3p mimics, and was reversed re-enhanced by co-transfecting FBXL3 expression vector (Fig. 5I). At last, cell migration and invasion promoted by miR-4735-3p overexpression were partially suppressed by FBXL3 overexpression (Fig. 5J).

4. Discussion

Non-small cell lung cancer (NSCLC) is one of the most common form of lung cancer [23]. More than thousands of new prevalence-incidence cases of patients with NSCLC was reported annually [21]. Reports showed that the delay of diagnosis of NSCLC patients or metastatic property was the major difficulty for the clinical therapy of NSCLC [22].

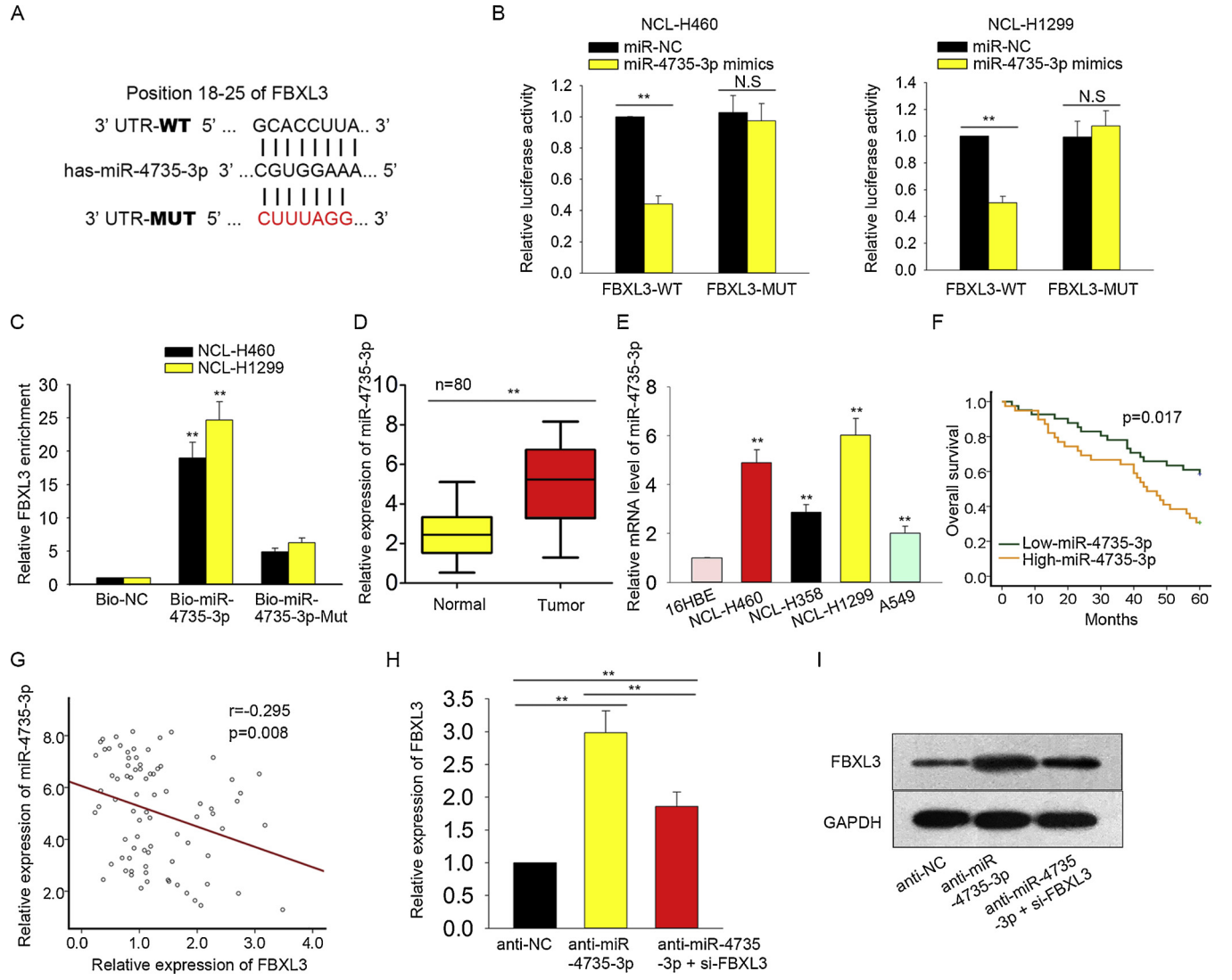

Fig. 4. MiR-4735-3p is an upstream modulator of FBXL3 in NSCLC. (A) The binding site between miR-4735-3p and FBXL3 was exhibited. (B) The luciferase activity was examined in NCL-H460 and NCL-H1299 cells co-transfected with miR-4735-3p mimic and pmiRGLO-3′-UTR-FBXL3-WT (FBXL3-WT) or miR-4735-3p mimic and pmiRGLO-3′-UTR-FBXL3-MUT (FBXL3-MUT). (C) The interaction between miR-4735-3p and FBXL3 was verified by RNA pull-down assay (D) The expression of miR-4735-3p in 80 pairs of NSCLC tissues and adjacent normal tissues was measured by qRT-PCR assay. (E) MiR-4735-3p expression was examined by qRT-PCR assay in NSCLC cell lines (NCL-H460, NCL-H358, NCL-H1299 and NCL-H146) and one normal bronchial epithelial cell line (16HBE). (F) Kaplan–Meier survival curve and log rank test were utilized to detect the association between miR-4735-3p expression and overall survival rate of NSCLC patient. (G) Spearman's correction analysis revealed the correlation between FBXL3 expression and miR-4735-3p expression. (H–I) The mRNA and protein levels of FBXL3 were detected in NSCLC cell transfected with anti-NC, anti-miR-4735-3p or anti-miR-4735-3p + si-FBXL3. ** $p <$ 0.01. N.S: no significance.

Till now, few effective therapeutic treatment and prevention method were found [20].

FBXL3 has been reported in human malignant cancers as a potential tumor suppressor, except for NSCLC. In this study, we detected the role of FBXL3 in NSCLC. The expression level of FBXL3 was found to be lower in NSCLC tissues and cell lines. Previous report has revealed that dysregulation of mRNA is correlated with the prognosis of cancer patients [25]. In the present study, we analyzed the correlation between FBXL3 expression and the clinicopathological features of NSCLC patients. The expression of FBXL3 was correlated with TNM stage. More importantly, the downregulation of FBXL3 correlated with the low overall survival of NSCLC patients. Therefore, we confirmed that FBXL3 might involve in NSCLC progression. Functionally, mRNAs can regulate various biological processes, such as cell proliferation, apoptosis and migration [9,24]. In this study, we detected the functions of FBXL3 in regulating NSCLC cell proliferation and migration. Interestingly, overexpression of FBXL3 efficiently suppressed cell proliferation, induced cell apoptosis and led to cell cycle arrest. Moreover, the cell migration, invasion and EMT process were found to be inhibited by FBXL3 overexpression.

Mechanistically, mRNAs can interact with miRNAs to regulate tumorigenesis and tumor progression [17–19,28]. MiRNAs are frequently dysregulated in NSCLC [1,7,30] and are able to regulate various biological processes, such as cell proliferation, migration and invasion [5,8,13]. Therefore, in our present study, we investigated the miRNA which cold interact with FBXL3 in NSCLC. Based on bioinformatics analysis, dual-luciferase report assay and pull-down assay, mechanism investigation demonstrated that miR-4735-3p was able to bind to FBXL3 3′UTR and negatively regulated FBXL3 in NSCLC. Similarly, we analyzed the correlation between miR-4735-3p expression and the overall survival rate of NSCLC patients. High expression level of miR-4735-3p was associated with the low overall survival rate of NSCLC patients. Finally, rescue assays demonstrated that miR-4735-3p promoted NSCLC progression, while the function of miR-4735-3p was

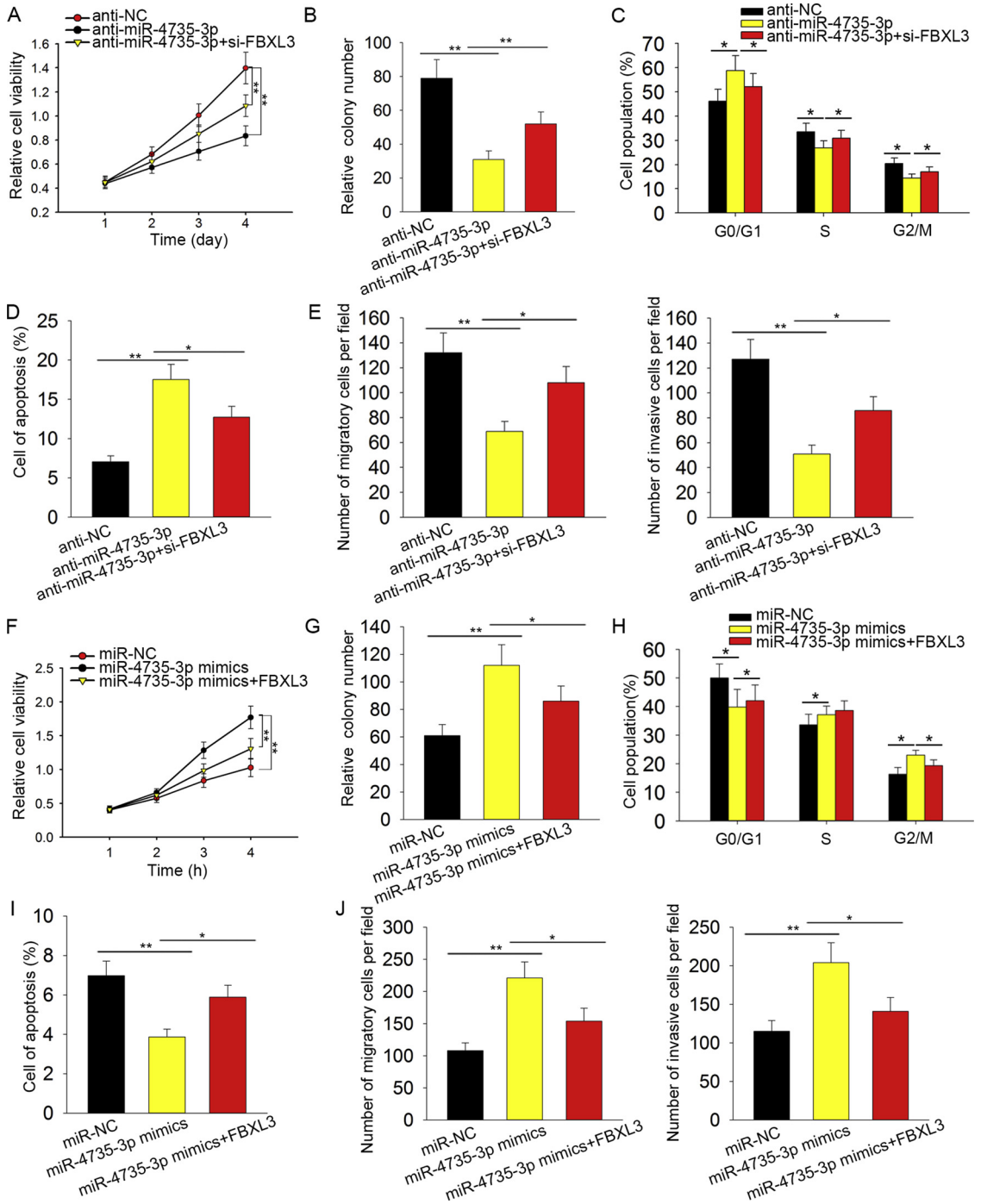

Fig. 5. MiR-4735-3p interacted with FBXL3 to regulate NSCLC progression. (A–B) Effects of FBXL3 knockdown on miR-4735-3p inhibitor-mediated NSCLC cell proliferation was detected by MTT and colony formation assay. (C–D) Cell cycle and apoptosis were measured by flow cytometry analysis when NSCLC cells were co-transfected with anti-miR-4735-3p or anti-miR-4735-3p and si-FBXL3. (E) Cell migration and invasion ability were detected by transwell assay after NSCLC cell co-transfected with anti-miR-4735-3p or anti-miR-4735-3p and si-FBXL3. (F–G) Cell proliferation was examined in cells transiently transfected with miR-NC, miR-4735-3p mimics or in cells co-transfected with miR-4735-3p mimics and FBXL3 expression vector. (H–I) Cell cycle distribution and cell apoptosis were detected in cells transiently transfected with miR-NC, miR-4735-3p mimics or in cells co-transfected with miR-4735-3p mimics and FBXL3 expression vector. (*J*) Transwell migration and invasion assays were conducted in cells transiently transfected with miR-NC, miR-4735-3p mimics or in cells co-transfected with miR-4735-3p mimics and FBXL3 expression vector. * $p < 0.05$; ** $p < 0.01$.

attenuated by FBXL3, indicating that miR-4375-3p interacted with FBXL3 to regulate NSCLC progression. All our findings suggested that FBXL3 was regulated by miR-4735-3p and acted as a tumor suppressor in NSCLC. Our research findings revealed that miR-4735-3p and FBXL3 may be two diagnostic or therapeutic targets for NSCLC, which will contribute to enrich the therapeutic strategy for NSCLC.

References

[1] M. Boeri, U. Pastorino, G. Sozzi, Role of microRNAs in lung cancer: microRNA signatures in cancer prognosis, Cancer J. (Sudbury, Mass.) 18 (2012) 268–274.

[2] C.M. Calvano Filho, D.C. Calvano-Mendes, K.C. Carvalho, G.A. Maciel, M.D. Ricci, A.P. Torres, J.R. Filassi, E.C. Baracat, Triple-negative and luminal a breast tumors: differential expression of miR-18a-5p, miR-17-5p, and miR-20a-5p, Tumour Boil.: J. Int. Soc. Oncodev. Biol. Med. 35 (2014) 7733–7741.

[3] G. Chen, Z.L. Shen, L. Wang, C.Y. Lv, X.E. Huang, R.P. Zhou, Hsa-miR-181a-5p expression and effects on cell proliferation in gastric cancer, Asian Pac. J. Cancer Prev.: APJCP 14 (2013) 3871–3875.
[4] W. Chen, R. Zheng, P.D. Baade, S. Zhang, H. Zeng, F. Bray, A. Jemal, X.Q. Yu, J. He, Cancer statistics in China, 2015, CA: Cancer J. Clin. 66 (2016) 115–132.
[5] X. Chen, A. Wang, X. Yue, miR-449c inhibits migration and invasion of gastric cancer cells by targeting PFKFB3, Oncol. Lett. 16 (2018) 417–424.
[6] D. Chu, J. Li, H. Lin, X. Zhang, H. Pan, L. Liu, T. Yu, M. Yan, M. Yao, Quantitative proteomic analysis of the miR-148a-associated mechanisms of metastasis in non-small cell lung cancer, Oncol. Lett. 15 (2018) 9941–9952.
[7] D. Cortinovis, V. Monica, F. Pietrantonio, G.L. Ceresoli, C.M. La Spina, L. Wannesson, MicroRNAs in non-small cell lung cancer: current status and future therapeutic promises, Curr. Pharm. Des. 20 (2014) 3982–3990.
[8] S. Deng, H. Wang, H. Fan, L. Zhang, J. Hu, Q. Tang, Z. Shou, X. Liu, D. Zuo, J. Yang, M. Xu, Q. Chen, Y. Dong, Z. Nan, H. Wu, Y. Liu, Over-expressed miRNA-200b ameliorates ulcerative colitis-related colorectal cancer in mice through orchestrating epithelial-mesenchymal transition and inflammatory responses by channel of AKT2, Int. Immunopharmacol. 61 (2018) 346–354.
[9] A. Gonzalez-Torres, E.G. Banuelos-Villegas, N. Martinez-Acuna, E. Sulpice, X. Gidrol, L.M. Alvarez-Salas, MYPT1 is targeted by miR-145 inhibiting viability, migration and invasion in 2D and 3D HeLa cultures, Biochem. Biophys. Res. Commun. (2018).
[10] X. Guo, Y. Zhu, X. Hong, M. Zhang, X. Qiu, Z. Wang, Z. Qi, X. Hong, miR-181d and c-myc-mediated inhibition of CRY2 and FBXL3 reprograms metabolism in colorectal cancer, Cell Death Dis. 8 (2017) e2958.
[11] R.S. Herbst, J.V. Heymach, S.M. Lippman, Lung cancer, New Engl. J. Med. 359 (2008) 1367–1380.
[12] M. Hollis, K. Nair, A. Vyas, L.S. Chaturvedi, S. Gambhir, D. Vyas, MicroRNAs potential utility in colon cancer: early detection, prognosis, and chemosensitivity, World J. Gastroenterol. 21 (2015) 8284–8292.
[13] Q. Hu, K. Du, X. Mao, S. Ning, miR-197 is downregulated in cervical carcinogenesis and suppresses cell proliferation and invasion through targeting forkhead box M1, Oncol. Lett. 15 (2018) 10063–10069.
[14] L. Hua, G. Zhu, J. Wei, MicroRNA-1 overexpression increases chemosensitivity of non-small cell lung cancer cells by inhibiting autophagy related 3-mediated autophagy, Cell Biol. Int. (2018).
[15] T. Kishikawa, M. Otsuka, M. Ohno, T. Yoshikawa, A. Takata, K. Koike, Circulating RNAs as new biomarkers for detecting pancreatic cancer, World J. Gastroenterol. 21 (2015) 8527–8540.
[16] B.P. Lewis, C.B. Burge, D.P. Bartel, Conserved seed pairing, often flanked by adenosines, indicates that thousands of human genes are microRNA targets, Cell 120 (2005) 15–20.
[17] H. Li, C. Feng, S. Shi, miR-196b promotes lung cancer cell migration and invasion through the targeting of GATA6, Oncol. Lett. 16 (2018) 247–252.
[18] B. Liu, J. Li, M. Zheng, J. Ge, J. Li, P. Yu, MiR-542-3p exerts tumor suppressive functions in non-small cell lung cancer cells by upregulating FTSJ2, Life Sci. 188 (2017) 87–95.
[19] S. Liu, Y. Yang, L. Chen, D. Liu, H. Dong, MicroRNA-154 functions as a tumor suppressor in non-small cell lung cancer through directly targeting B-cell-specific moloney murine leukemia virus insertion site 1, Oncol. Lett. 15 (2018) 10098–10104.
[20] Z. Lu, Y. Li, Y. Che, J. Huang, S. Sun, S. Mao, Y. Lei, N. Li, N. Sun, J. He, The TGFbeta-induced lncRNA TBILA promotes non-small cell lung cancer progression in vitro and in vivo via cis-regulating HGAL and activating S100A7/JAB1 signaling, Cancer Lett. 432 (2018) 156–168.
[21] L. Lv, J.Q. Jia, J. Chen, The lncRNA CCAT1 upregulates proliferation and invasion in melanoma cells via suppressing miR-33a, Oncol. Res. 26 (2018) 201–208.
[22] Y.B. Meng, X. He, Y.F. Huang, Q.N. Wu, Y.C. Zhou, D.J. Hao, Long noncoding RNA CRNDE promotes multiple myeloma cell growth by suppressing miR-451, Oncol. Res. 25 (2017) 1207–1214.
[23] L. Qi, F. Liu, F. Zhang, S. Zhang, L. Lv, Y. Bi, Y. Yu, lncRNA NEAT1 competes against let-7a to contribute to non-small cell lung cancer proliferation and metastasis, Biomed. Pharmacother. 103 (2018) 1507–1515.
[24] H. Qin, W. Liu, MicroRNA-99a-5p suppresses breast cancer progression and cell-cycle pathway through downregulating CDC25A, J. Cell. Physiol. (2018).
[25] F. Shen, H. Zheng, L. Zhou, W. Li, J. Liu, X. Xu, Identification of CD28 and PTEN as novel prognostic markers for cervical cancer, J. Cell. Physiol. (2018).
[26] S. Shrestha, S.D. Hsu, W.Y. Huang, H.Y. Huang, W. Chen, S.L. Weng, H.D. Huang, A systematic review of microRNA expression profiling studies in human gastric cancer, Cancer Med. 3 (2014) 878–888.
[27] R.L. Siegel, K.D. Miller, A. Jemal, Cancer Statistics, CA. Cancer J. Clin. 67 (2017) 7–30.
[28] L. Song, L. Peng, S. Hua, X. Li, L. Ma, J. Jie, D. Chen, Y. Wang, D. Li, miR-144-5p enhances the radiosensitivity of Non-small-cell lung cancer cells via targeting ATF2, Biomed Res. Int. 2018 (2018) 5109497.
[29] Y. Tang, G. Xiao, Y. Chen, Y. Deng, LncRNA MALAT1 promotes migration and invasion of non-small-cell lung cancer by targeting miR-206 and activating Akt/mTOR signaling, Anticancer Drugs (2018).
[30] I. Vannini, F. Fanini, M. Fabbri, MicroRNAs as lung cancer biomarkers and key players in lung carcinogenesis, Clin. Biochem. 46 (2013) 918–925.
[31] S.L. Wood, M. Pernemalm, P.A. Crosbie, A.D. Whetton, Molecular histology of lung cancer: from targets to treatments, Cancer Treat. Rev. 41 (2015) 361–375.
[32] F. Yang, K. Wei, Z. Qin, W. Liu, C. Shao, C. Wang, L. Ma, M. Xie, Y. Shu, H. Shen, MiR-598 suppresses invasion and migration by negative regulation of derlin-1 and epithelial-mesenchymal transition in non-small cell lung cancer, Cell. Physiol. Biochem. 47 (2018) 245–256.
[33] J. Zhang, D. Liu, Z. Feng, J. Mao, C. Zhang, Y. Lu, J. Li, Q. Zhang, Q. Li, L. Li, MicroRNA-138 modulates metastasis and EMT in breast cancer cells by targeting vimentin, Biomed. Pharmacother. 77 (2016) 135–141.